Recent Progress in Lunar Laser Ranging at Grasse Laser Ranging Station

Julien Chabé, Clément Courde, Jean-marie Torre, Sebastien Bouquillon, Adrien Bourgoin, Mourad Aimar, Dominique Albanese, Bertrand Chauvineau, Hervé Mariey, Gregoire Martinot-Lagarde, et al.

AGU100 ADVANCING EARTH AND SPACE SCIENCE

Earth and Space Science

RESEARCH ARTICLE
10.1029/2019EA000785

Special Section:
50 years of Apollo Science

Recent Progress in Lunar Laser Ranging at Grasse Laser Ranging Station

Julien Chabé[1], Clément Courde[1], Jean-Marie Torre[1], Sébastien Bouquillon[2], Adrien Bourgoin[2], Mourad Aimar[1], Dominique Albanèse[1], Bertrand Chauvineau[3], Hervé Mariey[1], Grégoire Martinot-Lagarde[1], Nicolas Maurice[1], Duy-Hà Phung[1], Etienne Samain[1], and Hervé Viot[1]

[1]Université Côte d'Azur, Observatoire de la Côte d'Azur, CNRS, IRD, Géoazur, Caussols, France, [2]SYRTE, Observatoire de Paris, Université PSL, CNRS, Sorbonne Université, LNE, Paris, France, [3]Université Côte d'Azur, Observatoire de la Côte d'Azur, CNRS, Laboratoire Lagrange, Nice, France

Abstract Based on a fully passive space segment, the lunar laser ranging experiment is the last of the Apollo Lunar Surface Experiments Package to operate. Observations from the Grasse lunar laser ranging station have been made on a daily basis since the first echoes obtained in 1981. In this paper, first, we review the principle and the technical aspects of lunar laser ranging. We then give a brief summary of the progress made at the Grasse laser ranging facility (Observatoire de la Côte d'Azur, Calern Plateau on the French Riviera) since the first echoes. The current performance, driven by the use of an infrared wavelength laser, is presented in the last section for the year 2018.

Key Points:
- The use of an infrared wavelength has improved the capacities of the Grasse lunar laser ranging station in terms of budget link, reflectors numbers, and synodic period observation
- The lunar laser ranging statistics from the Grasse station over the year 2018 are presented

Correspondence to:
J. Chabé,
chabe@oca.eu

Citation:
Chabé, J., Courde, C., Torre, J.-M., Bouquillon, S., Bourgoin, A., Aimar, M., et al. (2020). Recent progress in lunar laser ranging at Grasse laser ranging station. *Earth and Space Science*. 7, e2019EA000785. https://doi.org/10.1029/2019EA000785

Received 5 JUL 2019
Accepted 22 FEB 2020
Accepted article online 26 FEB 2020

1. Introduction

The Earth-Moon system is a gravity laboratory. A precise metrological link between these two bodies can probe the external and internal forces that rule their movements. Lunar laser ranging (LLR) is such a metrological link. LLR is sensitive to many parameters of many scientific fields (such as Earth-Moon dynamics, selenophysics, the lunar and terrestrial reference frames, Earth rotation parameters, and relativistic physics), and for a lot of these areas, the constraints provided by LLR are the strongest (Müller et al., 2019). As an example, many tests of gravitation have been achieved with the help of LLR (the equivalence principle, Lorentz symmetry, variation of the gravitational constant G, and post-Newtonian tests) by Nordtvedt (1968) or more recently by Bourgoin et al. (2017), Hofmann and Müller (2018), and Viswanathan et al. (2018). As a second example, LLR has provided several contributions to selenophysics due to the influence of the Moon interior on its librations (Bender et al., 1973; Williams et al., 1996, 2001) and more recently (Pavlov et al., 2016; Viswanathan et al., 2019; Williams & Boggs, 2015). Of course, efforts toward higher precision are essential to improve the scientific results (T. W. Murphy, 2013), but these must be accompanied by efforts to improve observability. To properly probe the Moon's orbit around Earth and its libration, measurements have to be made over the entire synodic period and on all available retroreflectors over a large time span (Rambaux & Williams, 2011). Technically, LLR consists of precisely measuring the time of flight of a laser pulse emitted from Earth toward a lunar reflector and reflected back to Earth, in order to achieve the most precise and accurate measurement of the Earth-Moon distance. However, pointing a telescope with arcsecond precision without a direct visual signal is rather difficult. Also, due to the relative motion of the reflector and the telescope, a pointing of the order of 1 arcsecond ahead of the reflector is needed. The difficulty of estimating atmospheric refraction correctly at low elevation angle is another obstacle to proper pointing toward the target. Atmospheric turbulence generates laser beam broadening, wandering, and speckle pattern formation, which randomizes the return signal. The illuminated surface of the Moon may submerge the signal into noise, which prevents most LLR stations from getting measurements around the time of the full moon.

The French project to get optical echoes from the lunar surface was launched in 1967 with the support of the Centre National de la Recherche Scientifique following the experiments made by the Massachusetts Institute of Technology (Smullin & Fiocco, 1962). However, the accuracy was limited to 100 m, due to the combined effects of the Moon relief and the size of the laser beam. The idea by the LURE team to use retroreflectors (Alley et al., 1965) gave a new direction to this project of building a laser ranging system for the Moon. In parallel, the Centre Nationale d'Etudes Spatiales started a collaboration with the USSR to build

the retroreflectors for the Lunokhod 1 and 2 rovers. On 21 July 1969, astronauts Neil Armstrong and Buzz Aldrin placed the first reflector panel on the lunar surface. The Lick Observatory succeeded in obtaining strong return signals from the Apollo XI reflector on 1 August (Faller et al., 1969). This first range measurement was made with an accuracy of 7 m. Soon afterward, McDonald Observatory successfully detected their first returns (Alley et al., 1970). Other range measurements were made at the Air Force Cambridge Research Laboratories Lunar Ranging Observatory in Arizona (AFCRL, 1970) and the Tokyo Astronomical Observatory in Japan. On the night of 1 November 1969, a French team obtained returns from the Apollo XI reflector at Observatoire du Pic du Midi with a ruby laser (26 J per 1 ms pulse) (Calame et al., 1970). This success convinced the French scientific community to build an instrument dedicated to LLR in a new observatory: The Centre d'Études Géodynamiques et Astronomiques (CERGA) was inaugurated in 1974 on the Calern plateau 20 km from the city of Grasse (French Riviera). CERGA was designed from the beginning as a laboratory for the development and testing of new instruments. The 20 km^2 semidesert karstic plateau of Calern has a high number of clear nights. The absence of mists and dust and the circulation of marine winds in horizontal layers due to the topography gives a stabilized atmosphere. The scientific activities covered by CERGA were diverse: astrometry, celestial mechanics, and space geodesy. Since then, the Grasse laser ranging station has been one of the leading LLR stations.

This paper is organized as follows: After reviewing the principle of LLR, we briefly discuss the local technical history of our LLR facility. Finally, after a discussion of the advantages of using infrared (IR) wavelength light, section 4 gives the current observation performance of the Grasse LLR station.

2. The Principle of LLR

The principle of LLR is to fire laser pulses toward target reflectors on the Moon and to detect the return signal. By measuring the time of flight of the light precisely, one can determine the distance between the laser ranging station and the corner cube reflector (CCR) on the lunar surface. However, this measurement is technically challenging. To have a non-negligible chance of detecting a return signal, the laser pulse energy must be relatively high (0.1 to 1 J). The outgoing laser beam from the telescope has a minimal divergence of about 1–3″ depending on the atmospheric turbulence (seeing conditions). The laser beam reaches a diameter of ≈6 km on the lunar surface so that only a fraction 10^{-9} of the light is reflected back by the CCR panel. On its way back to Earth, the divergence of the laser beam is >10″ and with a 1.54 m telescope, again only a fraction 10^{-9} of the light is collected. Because of other factors such as atmospheric transparency, atmospheric turbulence, and detector efficiency, the link budget measured experimentally is between 10^{-19} and 10^{-20}. In these conditions, it is only possible to detect returns from the CCR if the background noise is thoroughly filtered. Generally, the incoming photons in the telescope encounter three types of filter: A field filter rejects the photons that are coming from a direction far from the CCR's position, a tight spectral filter of 0.1 nm around the laser wavelength removes most of the background light from the lunar surface, and a time gate of about 100 ns is applied to the detectors around the expected return time. For an accuracy of 1 cm in the distance between the station and the target, one must measure the round-trip travel time of the laser pulse with an accuracy below 100 ps. To achieve this, the time measurement must be based on a very stable high-frequency signal such as that generated by a cesium or H-maser clock with a frequency stability better than 10^{-12}. Nevertheless, several other factors affect the precision, accuracy, and stability of the measurements. The distance is determined by using a model of the refractive index of the atmosphere based on local ground monitoring of the pressure, temperature, and humidity. The timing uncertainty generated by the lack of knowledge of the atmosphere can induce a time delay of 15 to 70 ps. The detectors at the station are not perfect, and their timing jitter can generate an uncertainty of several millimeters depending on the technology used. The cross-axis point of the telescope (the only point that stays fixed while the telescope is tracking the Moon) must be positioned with an accuracy below 1 cm in the Earth's reference frame. The Moon itself by its libration generates an oscillation of the orientation of the CCR panel that can spread the return signal from 0 to 350 ps (Samain et al., 1998). To face this technical challenge, an LLR station must monitor on a daily basis all kinds of bias, noise, and drifts that might arise from any of the subsystems (laser, clock, detectors, mechanical and optical drift, etc.).

At the Grasse LLR station, LLR observations are performed one reflector at a time, and each observation typically lasts for 10 min. During this time span, the time differences (residuals) between the predicted and the observed time of flight of the emitted photons are recorded. The predictions are provided each day

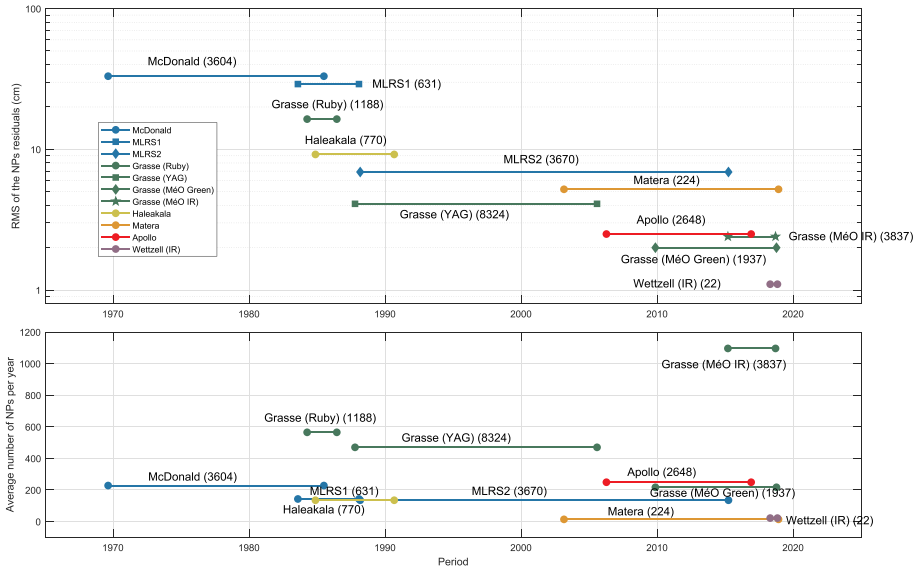

Figure 1. Achieved rms of the NP residuals for each configuration of LLR stations as a function of time (top). Average number of normal points acquired per year over the considered time spans (bottom). Data and statistics from POLAC (http://polac.obspm.fr/llrdata.html).

by the Paris Observatory Lunar Analysis Center (POLAC) in Topocentric Prediction Format for the LLR observations of the coming night. They are computed for all CCRs (and close craters) at two wavelengths (green and IR) with the most up-to-date Earth orientation parameters provided by the International Earth Rotation and Reference Systems Service. To separate the signal from the noise and to increase the precision of the measurement, a series of individual-shot observations is consolidated into a single representative launch time and associated with a round-trip travel time. (This consolidation can be done because the dynamics of the Earth-Moon system within this short time span is not of interest to LLR science.) These measurements, paired together with representative meteorological information and other auxiliary data, are packaged into a data unit called a normal point (NP).

3. Performance and Technical Evolution of LLR at the Grasse Station

Figure 1 shows the average number of NPs obtained per year and the rms of the NP residuals for each configuration of all LLR stations since 1969. The residuals have been obtained by POLAC by simulating the time of flight of the laser pulses with the LLR reduction software CAROLL, which now uses the ELPN lunar ephemeris (Bourgoin, 2016). The rms of the NP residuals given in Figure 1 is presented as a one-way distance after a 4-sigma cutoff. In what follows, we chose the residual rms as the estimator of the quality of the NPs instead of the NP intrinsic precision for two reasons. Firstly, it allows us to compare the quality of NPs taken by different stations at different epochs homogeneously, which is not possible with the available NP intrinsic precisions measured by different and not documented methods. Moreover, as the measurement of the NP intrinsic precision is based on the dispersion of its individual shots, it cannot be estimated a posteriori without the raw data. Secondly, most of the calibration biases are observable in the rms of the residuals and not in the NP intrinsic precision (bias in time reference, in the calibration of the cross-axis point of the telescope, etc.). However, it is important to keep in mind exactly what is plotted in this figure in order not to overinterpret or misinterpret it. For instance, the low rms of the Wettzell NP residuals is mainly due to the low number of NPs and is overoptimistic as an estimator of their quality, while the small rms difference between Grasse and Apollo is insignificant in comparison with model uncertainty.

The first LLR observations from the Grasse station (a 1.54 m Alt-Az Ritchey-Chrétien telescope) started in 1981, using a ruby laser ($\lambda = 684.3$ nm) firing 3 ns wide pulses of 3 J every 6 s. Over 4 years, 1,188 measurements were made, and the residual rms achieved was about 16.4 cm. In 1986, this success convinced the scientists involved to move toward a neodymium-doped yttrium aluminum garnet (Nd:YAG) laser emitting in the IR at a wavelength $\lambda = 1,064$ nm. Utilizing the second harmonic generation frequency doubling

method to reach a wavelength of 532 nm enabled the use of precise and less noisy detectors. The available energy per pulse was about 75 mJ in the green at a rate of 10 Hz, leading to a return rate of about one every 10 s. From 1986 to 2005, the Grasse station generated 8,324 NPs and reached a residual rms of 4.1 cm. This laser technology is still used today, but other kinds of improvement have been made during the last decade. In 2005, the station was upgraded by extending the operability of the MéO telescope to low Earth orbit satellites and improving the stability of the time base of the station for time transfer experiments, for example, Time Transfer by Laser Link (T2L2) on board the Jason-2 satellite. Several upgrades were made to the electronics, and new event timers and a fibered calibration system were installed. In 2012, the pulse duration at the Grasse station was increased from less than 70 to 150 ps by replacing the hazardous dye saturable absorber with a 4-mm-thick MolTech GmbH Cr4+:YAG crystal (Martinot-Lagarde et al., 2016). This modification reduced and simplified the routine maintenance of the laser system and was beneficial for the operability of the laser ranging facility. In this last period, with only the green wavelength laser, the NP residual rms was about 2.0 cm.

4. Current LLR Performance at the Grasse Station

4.1. The Infrared Wavelength

In 2015, a major upgrade was made at the Grasse LLR station to use directly the native IR wavelength of the Nd:YAG laser directly (Courde et al., 2017). The progress made in InGaAs technology prompted the station to purchase an InGaAs/InP single-photon avalanche diode. The quantum efficiency of this detector is about 20% in Geiger mode at $\lambda = 1{,}064$ nm, and the active area has a diameter of 80 μm. With a measured timing jitter of about 109 ps full width at half maximum, the level of precision is suitable for LLR.

LLR observations in the IR from the Grasse station constitute almost all observations since the implementation of this detector. Courde et al. show that performing LLR in the IR increases the station efficiency by a factor of 8 during new and full moon periods and improves the temporal homogeneity of the LLR observations over a synodic month. There are three main reasons for these improvements in performance. First of all, the number of photons is increased by a factor of 3. Next, there is better atmospheric transmission in the IR; for example, in a clear atmosphere, the transmission is improved by a factor of 1.9 at an elevation angle of 20° and by 1.32 at 40° (Degnan, 2013). And finally, the far-field diffraction pattern from a CCR is twice as large in the IR. Taking into account a typical 5 μrad velocity aberration, the relative gain in intensity between IR and green is 1.3 on Apollo arrays and 2.1 on Lunokhod arrays (Courde et al., 2017). Also, because of the transmittance and the scattering effects in the atmosphere, the solar noise is less important in the IR than in green light for elevation angles greater than 30°. All these properties of the IR naturally extend the capability of the station to range the lunar reflectors at lower elevation angles and closer to the new moon and full moon.

Along with the use of an IR laser, some technical improvements made at the station have been beneficial for our LLR performances, so that the number of NPs has jumped during 2018 with a one-way NP residual rms of 2.4 cm in 2018. First, beam divergence has been carefully calibrated and controlled for both wavelengths. Then, the laser coudé path of the telescope is now carefully tuned to avoid pointing errors in the emergent laser beam for different azimuth angles. Finally, a mechanical correction on the M3 mirror position of the telescope (Ritchey-Chrétien design) has been made to correct residual optical aberrations. This clearly improved the link budget during the year 2018, and some NPs have been acquired with more than 1.5 returns per second. Figure 2 shows an example of a ranging session on the Apollo XI retroreflector while the sky was clear and the seeing value was 0.97″; 465 returns were obtained while the Moon was at 25° elevation and the retroreflector panel was illuminated.

The recent contribution of the Wettzell laser ranging station to LLR (see Figure 1) is interesting as this station also now uses the IR wavelength but with a pulse duration of 20 ps, which explains the good NP residual rms they obtained. However, the 1 cm rms attributed by POLAC to this station has to be confirmed since this rms computation is based on only 22 NPs (spread over only six nights and for only two CCRs).

4.2. Observation Statistics Over 2018

In this section, we present the data collected from 1 January 2018 to 11 September 2018, the final day before our last IR single-photon avalanche diode broke. Even though the statistics are based on less than a year's worth of data, the number of NPs collected reached 973, a good performance in LLR history.

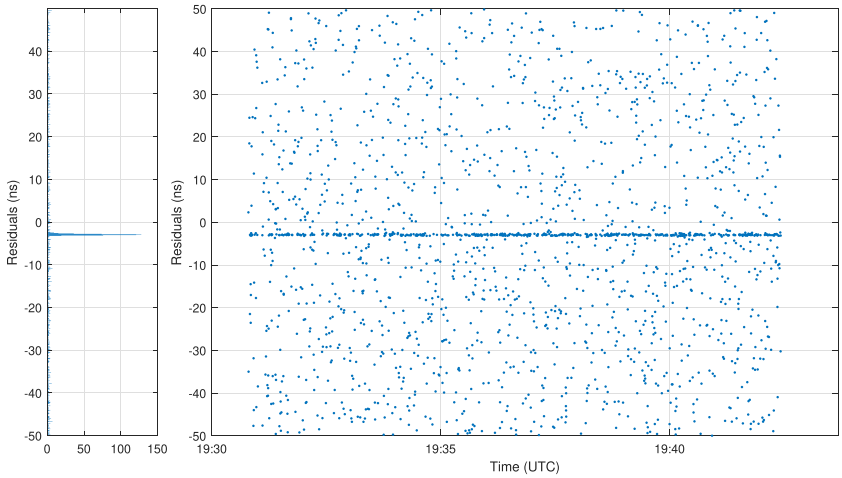

Figure 2. Example of a ranging session on the Apollo XI reflector panel on 23 July 2018; 465 returns were obtained and used to generate an NP.

The observation strategy of the Grasse station gives a high priority to LLR compared to other stations from the ILRS network. When the weather is good enough, an LLR session starts when the Moon's elevation is above 20°. Below 20°, air-mass transmission and atmospheric turbulence drastically reduce the probability of acquiring returns. However, thanks to the IR wavelength, and if the atmosphere is clear and the seeing exceptional ($\epsilon_0 < 1''$), data can be acquired below 20° and some operators try their luck. Apollo XV is always the first reflector ranged in order to evaluate the link budget, then Lunokhod 1, Lunokhod 2, Apollo XI, and Apollo XIV.

Figure 3 shows the percentage of acquired NPs for each reflector over three separate years. The green wavelength (2014) suffered from a large inhomogeneity in the reflectors observed, with very few NPs from the French reflectors on the Soviet rovers. Statistics at the IR wavelength (2017 and 2018) are much better. Operating in the IR highlights an efficiency problem at the green wavelength for the Lunokhod retroreflectors, especially for Lunokhod 2, as described in Courde et al. (2017) and T. Murphy et al. (2011). In this case, the theoretical efficiency doesn't coincide with the observed efficiency. In 2018, we managed to reach an almost perfect homogeneity on the ranged reflectors over the year. This homogeneity is not only in the total of number of NPs but also throughout the lunar cycle as shown by Figure 4. This figure presents the number of ranged reflectors as a function of the lunar cycle. If we were able to acquire at least one NP at a given time in the lunar cycle from a reflector, it appears on this graph. Most of the time, we were able to probe the five reflectors, except around the full moon where the Lunokhod reflectors are not designed to operate (Fournet, 1972). This performance was reached during summer 2018, right after the technical modifications mentioned above, as can be seen in Figure 5.

Figure 5 gives an overview of the sampling of the observations over the year. The top panel shows the number of returns of each NP as a function of time. The middle one plots the elongation of the Moon as a function of time and the bottom one the elevation of the Moon as a function of time. One can see that during the major

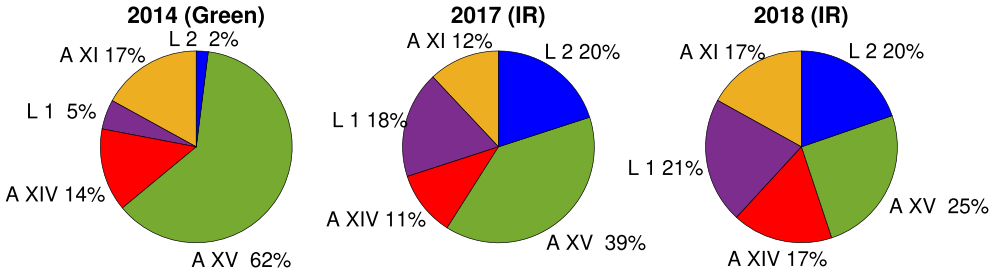

Figure 3. Retroreflector normal point statistics from the Grasse LLR station in 2014 (with only the green wavelength), 2017, and 2018.

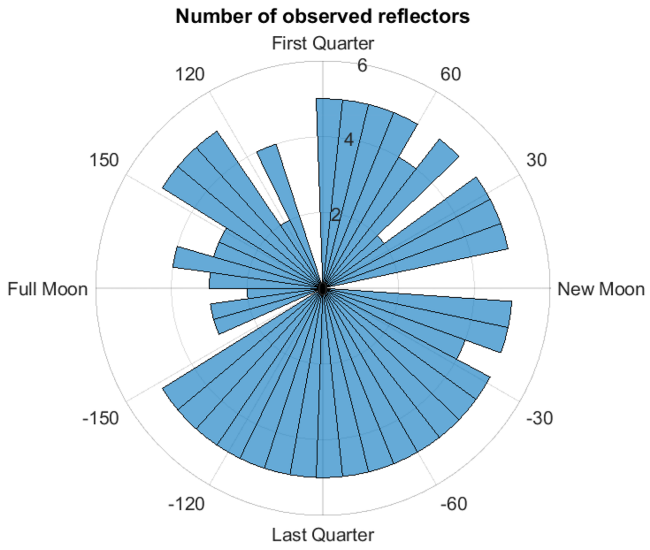

Figure 4. Number of reflectors observed as a function of the lunar cycle in 2018.

part of the year, good ranging sessions with more than 250 returns can be achieved around the first quarter at favorable elevations. Thanks to the small technical improvements mentioned, the summer season shows very good ranging sessions with more than 500 returns. While the sky is clear, this allows the entire lunar cycle to be ranged using almost all reflectors panels (red rectangle).

4.3. A Continuous Lunar Cycle Observation

During the summer of 2018, thanks to favorable weather and seeing conditions, we were able to range all reflectors through the entire lunar cycle with high signal-to-noise ratio (red rectangle in Figure 5). A total of 345 NPs were acquired in the IR during this lunar cycle, and some of them were generated with more than a thousand returns from the lunar surface in 10 min. A high-signal regime that has never been reached with the green wavelength before.

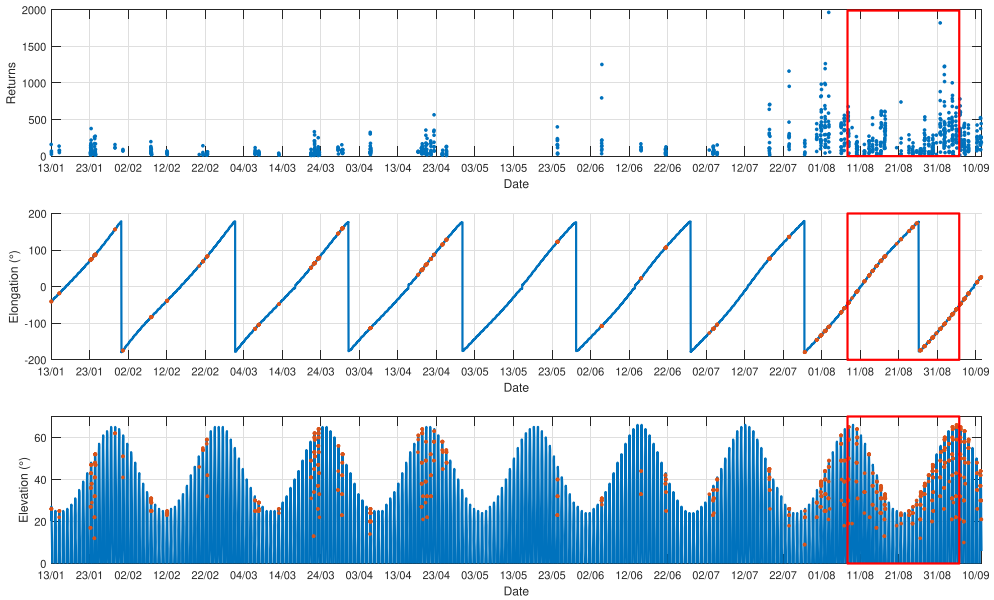

Figure 5. Overview of measurements over 2018. Top: number of returns as a function of time. Middle: elongation of the Moon as a function of time. Bottom: elevation of the Moon as a function of time. Red rectangle is the period detailed in 4.3.

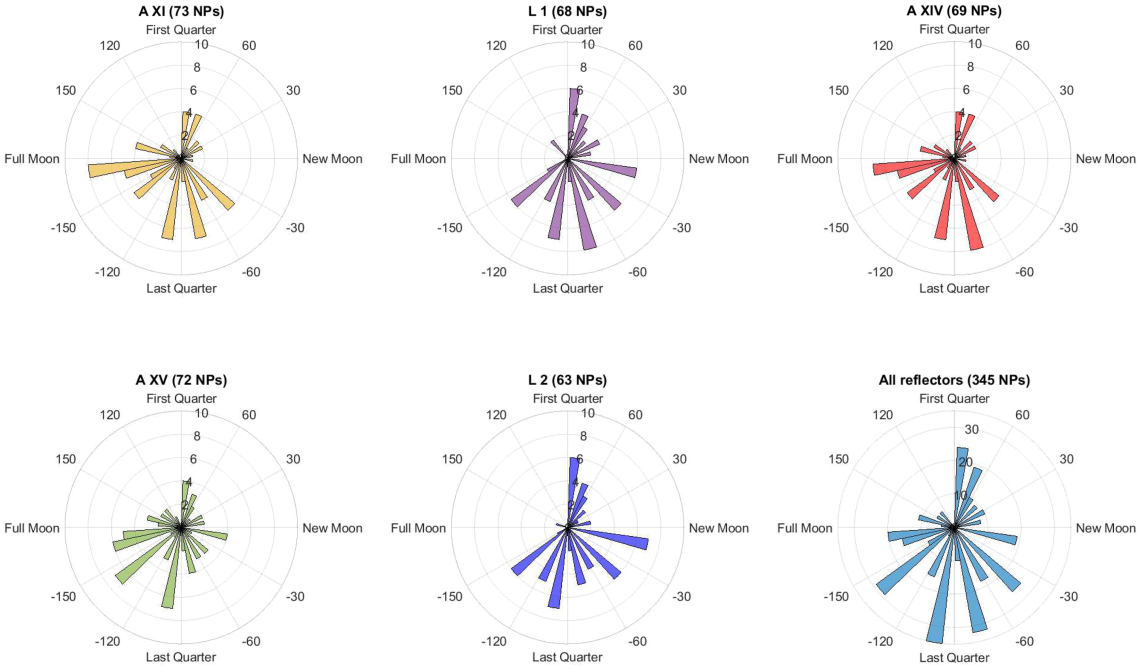

Figure 6. Normal point statistics for each reflector and all cumulated reflectors (bottom right corner) during a full lunar cycle from 8 August 2018 to 6 September 2018.

Between 8 August 2018 and 6 September 2018, the weather was clear. The night seeing had a median value of 0.8″ during this period. Figure 6 presents the NP statistics for each retroreflector (A XI, L 1, A XIV, A XV, and L 2) and for all the reflectors (bottom right corner) as a function of the lunar cycle.

Figure 7 helps to explain the observations of Figure 6. The histogram of total NPs as a function of the lunar cycle is plotted along with the elevation of the Moon because, on a single lunar cycle, the impact of the phase and elevation of the Moon on the LLR performance cannot be decoupled. The red dots show a series of measurements on the five reflectors. The lack of data immediately after the first quarter is due to a technical constraint. Also, before the full moon, the target was always below 30° elevation. The time available to range the reflectors was therefore reduced and the air-mass/turbulence effects decreased the signal-to-noise ratio, limiting the number of NPs that could be obtained.

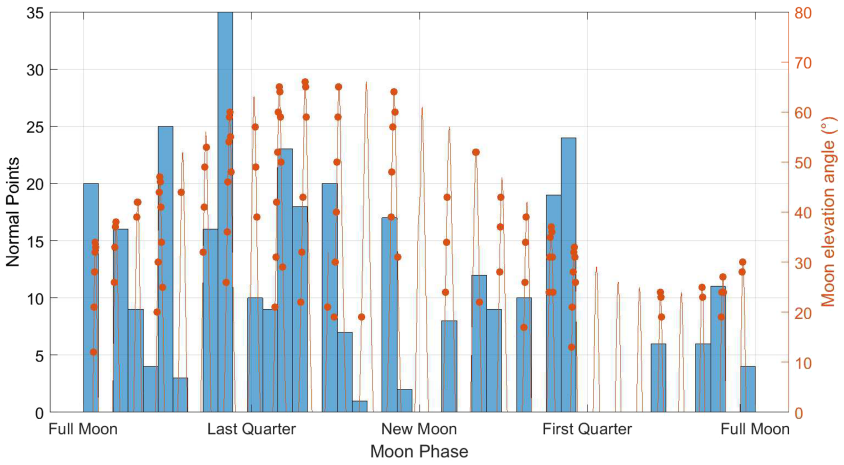

Figure 7. Normal point statistics for all reflectors during a full lunar cycle from 9 August 2018 to 6 September 2018. Each red dot represents a session with NPs obtained on the five retroreflectors, where each red dot is presented at its Moon elevation angle.

5. Conclusion

After a few years of LLR in the IR, the Grasse LLR station has improved its observational capabilities. The signal-to-noise ratio is greatly improved so that NP statistics cover almost all the synodic period. Measurements close to the new moon and full moon are possible, and almost all the reflectors are ranged over the lunar cycle; this is crucial in order to better resolve the physical libration effect and give information about the structure of the lunar interior. The link budget improvement is also interesting to study to compare the relative efficiency of the lunar reflectors and the lunar orbiter reflectors (Lunar Reconnaissance Orbiter, Queqiao). This will help to better understand the reflector degradation and sensitivity to solar radiation and the Moon environment (dust effect) (Currie et al., 2013; Goodrow & Murphy, 2012; Murphy & Goodrow, 2013). The performance in the IR is also very favorable for new monolithic CCRs, which are smaller but have a better ranging precision. A sparse network of large single corner cubes that could be resolved by a 100 ps laser pulse system would greatly improve the precision of LLR (Currie et al., 2013; Garattini et al., 2013). The use of the IR wavelength also increases the number of stations that could enter the LLR community. Sharing the data production with other stations will improve the lunar cycle sampling and can only be beneficial for the scientific outcomes from LLR. The most cost-effective experiment from the lunar exploration missions probably has some great scientific results to offer in the next few years.

Acknowledgments
This work is supported by Observatoire de la Côte d'Azur, CNRS Géoazur, CNRS-INSU under the National Observation Services program and CNES. Data are available from Crustal Dynamics Data Information System (https://cddis.nasa.gov/Data_and_Derived_Products/SLR/Normal_point_data.html) and from POLAC (http://polac.obspm.fr/llrdata.html). We would like to thank all the people who have been involved in the past in the French Lunar Laser Ranging program and the ILRS for its support.

References

AFCRL (1970). Report on research at AFCRL: July 1967 June 1970, AFCRL-71-0022, Air Force Cambridge Research Laboratory.
Alley, C. O., Bender, P. L., Dicke, R. H., Faller, J. E., Franken, P. A., Plotkin, H. H., & Wilkinson, D. T. (1965). Optical radar using a corner reflector on the Moon. *Journal of Geophysical Research*, *70*(9), 2267–2269.
Alley, C. O., Chang, R. F., Currie, D. G., Mullendore, J., Poultney, S. K., Rayner, J. D., et al. (1970). Apollo 11 laser ranging retro-reflector: Initial measurements from the Mcdonald Observatory. *Science*, *167*(3917), 368–370.
Bender, P. L., Currie, D. G., Poultney, S. K., Alley, C. O., Dicke, R. H., Wilkinson, D. T., et al. (1973). The lunar laser ranging experiment. *Science*, *182*(4109), 229–238.
Bourgoin, A. (2016). Constraints on Lorentz symmetry violations using lunar laser ranging observations (Ph.D. Thesis), École Doctorale d'Astronomie et d'Astrophysique dîle-de-France.
Bourgoin, A., Le Poncin-Lafitte, C., Hees, A., Bouquillon, S., Francou, G., & Angonin, M. C. (2017). Lorentz symmetry violations from matter-gravity couplings with lunar laser ranging. *PRL*, *119*(20), 201102.
Calame, O., Fillol, M.-J., Guérault, G., Muller, R., Orszag, A., Pourny, J.-C., et al. (1970). Premiers échos lumineux sur la lune obtenus par le télémètre laser du pic du midi. *Comptes Rendus de l'Académie des Sciences/Paris*, *270*, 1637.
Courde, C., Torre, J., Samain, E., Martinot-Lagarde, G., Aimar, M., Albanese, D., et al. (2017). Lunar laser ranging in infrared at the Grasse laser station. *Astronomy & Astrophysics*, *602*, A90.
Courde, C., Torre, J., Samain, E., Martinot-Lagarde, G., Aimar, M., Albanese, D., et al. (2017). *Satellite and lunar laser ranging in infrared* (Vol. 10229). https://doi.org/10.1117/12.2270573
Currie, D. G., Dell-Agnello, S., Delle Monache, G. O., Behr, B., & Williams, J. G. (2013). A lunar laser ranging retroreflector array for the 21st century. *Nuclear Physics B - Proceedings Supplements*, *243-244*, 218–228.
Currie, D. G., Delle Monache, G., Dell'Agnello, S., & Murphy, T. (2013). Dust degradation of Apollo lunar laser retroreflectors and the implications for the next generation lunar laser retroreflectors. In *AGU Fall Meeting Abstracts*, *2013*, pp. P51G–1815.
Degnan, J. J. (2013). Contribution of space geodesy to geodynamics: Technology. 133.
Faller, J., Winer, I., Carrion, W., Johnson, T. S., Spadin, P., Robinson, L., et al. (1969). Laser beam directed at the lunar retro-reflector array: Observations of the first returns. *Science*, *166*(3901), 99–102.
Fournet, M. (1972). Le réflecteur laser de Lunokhod.
Garattini, M., Dell Agnello, S., Currie, D., Delle Monache, GO., Tibuzzi, M., Patrizi, G., et al. (2013). Moonlight: A new lunar laser ranging retroreflector instrument. *Acta Polytechnica*, *53*(A), 821–824.
Goodrow, S. D., & Murphy, T. W. (2012). Effects of thermal gradients on total internal reflection corner cubes. *Applied Optics*, *51*(36), 8793–8799.
Hofmann, F., & Müller, J. (2018). Relativistic tests with lunar laser ranging. *Classical and Quantum Gravity*, *35*(3), 035015.
Martinot-Lagarde, G., Aimar, M., Alban Ese, D., Courde, C., Exertier, P., Fienga, A., et al. (2016). Laser enhancements for lunar laser ranging at 532 nm. *Results in Physics*, *6*, 329–336.
Müller, J., Murphy, T. W., Schreiber, U., Shelus, P. J., Torre, J.-M., Williams, J. G., et al. (2019). Lunar laser ranging: A tool for general relativity, lunar geophysics and earth science. *Journal of Geodesy*, *93*, 2195–2210.
Murphy, T. W. (2013). Lunar laser ranging: The millimeter challenge. *Reports on Progress in Physics*, *76*(7), 076901.
Murphy, T. W., Adelberger, E. G., Battat, J. B. R., Hoyle, C. D., Johnson, N. H., McMillan, R. J., et al. (2011). Laser ranging to the lost Lunokhod 1 reflector. *Icarus*, *211*(2), 1103–1108.
Murphy, T. W., & Goodrow, S. D. (2013). Polarization and far-field diffraction patterns of total internal reflection corner cubes. *Applied Optics*, *52*(2), 117–126.
Nordtvedt, K. (1968). Testing relativity with laser ranging to the moon. *Physical Review*, *170*, 1186–1187.
Pavlov, D. A., Williams, J. G., & Suvorkin, V. V. (2016). Determining parameters of Moon's orbital and rotational motion from LLR observations using GRAIL and IERS-recommended models. *Celestial Mechanics and Dynamical Astronomy*, *126*(1-3), 61–88.
Rambaux, N., & Williams, J. G. (2011). The Moon's physical librations and determination of their free modes. *Celestial Mechanics and Dynamical Astronomy*, *109*(1), 85–100.
Samain, E., Mangin, J. F., Veillet, C., Torre, J. M., Fridelance, P., Chabaudie, J. E., et al. (1998). Millimetric lunar laser ranging at OCA (Observatoire de la Côte d'Azur). *Astronomy and Astrophysics Supplement Series*, *130*(2), 235–244.
Smullin, L. D., & Fiocco, G. (1962). Optical echoes from the moon. *Nature*, *194*(4835), 1267–1267.

Viswanathan, V., Fienga, A., Minazzoli, O., Bernus, L., Laskar, J., & Gastineau, M. (2018). The new lunar ephemeris INPOP17a and its application to fundamental physics. *mnras*, *476*, 1877–1888.

Viswanathan, V., Rambaux, N., Fienga, A., Laskar, J., & Gastineau, M. (2019). Observational constraint on the radius and oblateness of the lunar core-mantle boundary. *Geophysical Research Letters*, *46*, 7295–7303. https://doi.org/10.1029/2019GL082677

Williams, J. G., & Boggs, D. H. (2015). Tides on the Moon: Theory and determination of dissipation. *Journal of Geophysical Research: Planets*, *120*, 689–724. https://doi.org/10.1002/2014JE004755

Williams, J. G., Boggs, D. H., Yoder, C. F., Ratcliff, J. T., & Dickey, J. O. (2001). Lunar rotational dissipation in solid body and molten core. *Journal of Geophysical Research*, *106*(E11), 27933–27968.

Williams, J. G., Newhall, X., & Dickey, J. O. (1996). Lunar moments, tides, orientation, and coordinate frames. *Planetary and Space Science*, *44*(10), 1077–1080.